

Diffusion-Emission Theory of Photon Enhanced Thermionic Emission Solar Energy Harvesters

Aapo Varpula^{1, a)} and Mika Prunnila¹

VTT Technical Research Centre of Finland, P. O. Box 1000, FI-02044 VTT, Espoo, Finland

(Dated: 23 June 2018)

Numerical and semi-analytical models are presented for photon-enhanced-thermionic-emission (PETE) devices. The models take diffusion of electrons, inhomogeneous photogeneration, and bulk and surface recombination into account. The efficiencies of PETE devices with silicon cathodes are calculated. Our model predicts significantly different electron affinity and temperature dependence for the device than the earlier model based on a rate-equation description of the cathode. We show that surface recombination can reduce the efficiency below 10 % at the cathode temperature of 800 K and the concentration of 1000 suns, but operating the device at high injection levels can increase the efficiency to 15 %.

I. INTRODUCTION

Currently solar energy is converted to electric power using two technologies: photovoltaic (PV) solar cells and concentrated solar power systems based on heat engines¹. The former system requires low and the latter high operating temperatures. This discrepancy poses a challenge for combination of the two systems in tandem, where the heat engines exploit the waste heat of the PV system. A photon-enhanced-thermionic-emission (PETE) device proposed by Schwede et al.² is a PV device which benefits from high operation temperatures. It can be coupled to a heat engine, thereby allowing total efficiencies above 50% to be potentially reached.

The PETE device is depicted in Fig. 1. The photons are absorbed in the cathode, i.e. the absorber, which is a P-type semiconductor. The cathode material should have a suitably low energy gap so that most of the solar photons are absorbed. The absorbed photons are thermionically emitted from the cathode to vacuum, where they travel to the anode, i.e. the electron collector. The surface of the cathode should have a low electron affinity in order to have reasonably strong thermionic emission. Electron affinity can be tuned significantly below the bulk value by different surface coatings (see Refs. 2 and 12 and references therein). Even negative electron affinities can be obtained for silicon¹². These coatings, however, might not be stable at the high operation temperatures of PETE devices. The anode material can be metal or N-type semiconductor with suitably low work function in order to have high output voltage V for the device.

In the PETE device model of Ref. 2 the cathode material is described by a single rate equation that neglects many important effects, such as diffusion and realistic recombination. In this article, we present a model that takes the most of the relevant effects in semiconductors into account. We solve the electron density in the cathode numerically in the general case and derive also a

semi-analytical model, which can be used at low injection levels. Silicon is a good candidate for PETE due to its rather low band gap, good thermal stability, high availability, cost-efficiency, and good manufacturability. Therefore, we use our models to calculate the characteristics of a PETE device with a silicon cathode using experimentally verified material data. We find that at low temperatures our model predicts a significantly lower efficiency than the model presented in Ref. 2. The overall temperature and electron affinity dependency of the efficiency differs also from that of Ref. 2. Furthermore, we show that surface recombination can reduce the efficiency of the PETE device below 10 %, but operating the device at high injection levels can provide an enhancement where efficiency of 15 % is reached.

II. THEORY

A. Semiconductor material model

The Fermi level E_F is solved numerically using the electroneutrality condition³ $n_{eq} + N_A^- = p_{eq} + N_D^+$, where n_{eq} and p_{eq} are the densities of electrons and holes in the thermodynamical equilibrium, and N_A^- and N_D^+ are the densities of ionized acceptors and donors, respectively. For the temperature dependence of the band gap of silicon we use the standard formula³

$$E_g(T) = E_g(0) - \frac{\alpha_g T^2}{T + \beta_g}, \quad (1)$$

where $E_g(0) = 1.170$ eV, $\alpha_g = 4.73 \times 10^{-4}$ eV/K, and $\beta_g = 636$ K.

The total minority-electron lifetime in bulk can be written as⁴⁻⁶

$$\tau_n = \frac{1}{B(n + p_{eq}) + (C_n n + C_p p)(n + p_{eq}) + \frac{1}{\tau_{SRH}}}, \quad (2)$$

where B is the radiative recombination coefficient, n and p are the densities of electrons and holes, respectively, C_n and C_p are the Auger recombination coefficients for electrons and holes, respectively, and τ_{SRH}

^{a)}Electronic mail: aapo.varpula@vtt.fi

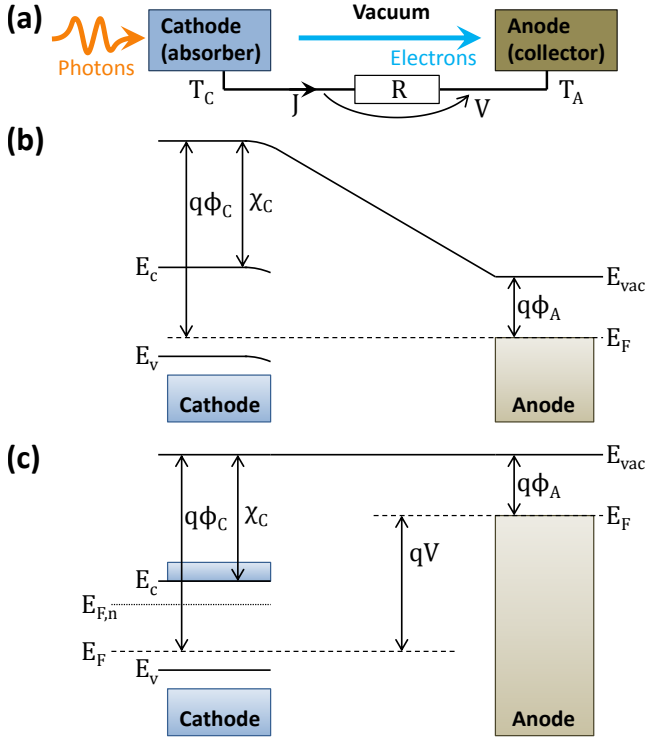


FIG. 1. (a) Schematic picture of the PETE device. T_C is the absolute temperature of cathode, T_A the absolute temperature of anode, V the output voltage, J the density of the output current, and R a resistor representing the external load. The energy bands of the device (b) in the thermodynamical equilibrium and (c) in the flat-band case, which often yields the highest power output. E_F is the Fermi level, $E_{F,n}$ is the quasi Fermi level of electrons, q is the elementary charge, χ_C is the electron affinity of the cathode, ϕ_C and ϕ_A are the work functions of the cathode and the anode, E_v is the valence band maximum, E_c is the conduction band minimum, and E_{vac} is the vacuum energy level. Here the anode is metal, but it can be an N-type semiconductor as well.

is the Shockley-Read-Hall (SRH) recombination lifetime, which is directly proportional to the density of the deep-level impurities in the material, and it increases when the injection level is increased⁵. The SRH lifetime has constant saturation values both in low and high injection regimes⁵. Therefore, we use constant $\tau_{SRH} = 2.5 \mu\text{s}$ to represent a high quality silicon⁶ at either low or high injection level. For silicon⁵ $B = 4.73 \times 10^{-15} \text{ cm}^3/\text{s}$ and $C_p = 10^{-31} \text{ cm}^6/\text{s}$, which is a value measured at low injection level. In a P-type material C_p determines the Auger lifetime in low and the ambipolar Auger coefficient $C_A = C_n + C_p$ in high injection conditions⁵, respectively. The experimental high-injection value for C_A differs from $C_n + C_p$ measured at low injection levels^{4,6}. We take the both injection regimes into account using an artificial value of $10^{-30} \text{ cm}^6/\text{s}$ for C_n . For electron mobility μ_n in silicon we use a model⁷ optimized for a wide temperature range. Mobility is linked to the diffusion coefficient $D_n = k_B T \mu_n / q$, where T is the absolute temperature

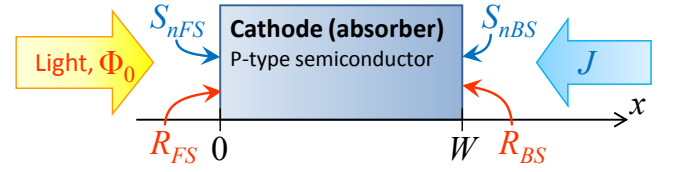


FIG. 2. Schematic picture of the cathode of the PETE device.

and q the elementary charge. For the absorption coefficient α of silicon we use a widely-used semi-empirical model^{8,9}.

B. Electron density

The electron density n in the cathode sketched in Fig. 2 can be calculated using the continuity equation, the generation and recombination rate equations, and the drift-diffusion current formulas for the charge carriers³. We assume that the electric field inside the cathode is approximately zero, because the most of the voltage difference is across the vacuum gap and the photogeneration of electron-hole pairs supports the local approximate charge neutrality. This simplifies the solution considerably, since holes need not to be taken into account explicitly. In addition, the band bending near the cathode surface (see Fig. 1b) is neglected, since the effect is small and the PETE device is mostly operated near the flat-band case (shown in Fig. 1c), where the band bending disappears. The excess-electron density $\Delta n(x) = n(x) - n_{eq}$ can be described by

$$\frac{d^2 \Delta n}{dx^2} = \frac{\Delta n}{L_n^2} - \frac{G_n(x) \tau_n}{L_n^2}, \quad (3)$$

where $L_n = \sqrt{D_n \tau_n}$ is the diffusion length of electrons and the generation is given by

$$G(x) = \alpha \Phi_0 (1 - R_{FS}) \left[e^{-\alpha x} + R_{BS} e^{\alpha(x-2W)} \right], \quad (4)$$

where α is the absorption coefficient, Φ_0 is the incident flux of photons, $R_{FS(BS)}$ is the front (back) surface reflection coefficient, and W is the thickness of the cathode. The boundary conditions are

$$\left. \frac{d\Delta n}{dx} \right|_{x=0} = \frac{S_{nFS}}{D_n} \Delta n(0) \quad (5)$$

$$\left. \frac{d\Delta n}{dx} \right|_{x=W} = -\frac{S_{nBS}}{D_n} \Delta n(W) - \frac{J}{qD_n}, \quad (6)$$

where $S_{nFS(BS)}$ is the front (back) surface recombination velocity and J is the density of the output current.

The analytical solution exist when τ_n is constant, which is valid at low injection levels (i.e. $\Delta n \ll p_{eq}$). Assuming the low-injection case and using Eqs. (5) and (6) the solution of Eq. (3) at $x = W$ is given by

$$\Delta n(W) = -\frac{L_n k}{qD_n} J + \Delta n_{\text{sun}}, \quad (7)$$

where

$$k = \frac{1}{a} \left[\cosh\left(\frac{W}{L_n}\right) + \frac{L_n S_{nFS}}{D_n} \sinh\left(\frac{W}{L_n}\right) \right], \quad (8)$$

$$a = \sinh\left(\frac{W}{L_n}\right) + \frac{L_n S_{nFS}}{D_n} \cosh\left(\frac{W}{L_n}\right) + \frac{b L_n S_{nBS}}{D_n}, \quad (9)$$

$$b = \cosh\left(\frac{W}{L_n}\right) + \frac{L_n S_{nFS}}{D_n} \sinh\left(\frac{W}{L_n}\right), \quad (10)$$

and

$$\begin{aligned} \Delta n_{\text{sun}} = & \int_0^\infty d\lambda \frac{\tau_n \alpha \Phi_0 (1 - R_{FS})}{1 - \alpha^2 L_n^2} \left(e^{-\alpha W} (1 + R_{BS}) \right. \\ & + \frac{L_n}{a} \left\{ -\frac{S_{nFS}}{D_n} - \alpha - R_{BS} e^{-2\alpha W} \left(\frac{S_{nFS}}{D_n} - \alpha \right) \right. \\ & \left. \left. + b e^{-\alpha W} \left[-\frac{S_{nBS}}{D_n} + \alpha - R_{BS} \left(\frac{S_{nBS}}{D_n} + \alpha \right) \right] \right\} \right), \quad (11) \end{aligned}$$

where λ is the wavelength of photons. The first term in Eq. (7) describes the fact that the electrons need to diffuse from bulk of the cathode to the back surface in order to be emitted. When current is drawn, $\Delta n(W)$ will decrease because of this diffusion process. The second term in Eq. (7) represents the excess electrons due to the photogeneration.

C. Output current

The density of the cathode current, which corresponds to electrons emitted from the cathode, can be written using the quasi Fermi level $E_{F,n} = E_F + k_B T_C \ln(n/n_{eq})$ as

$$J_C = A_C^* T_C^2 \exp\left(-\frac{\Delta E_C}{k_B T_C}\right) \frac{n}{n_{eq}}, \quad (12)$$

where $\Delta E_C = q\phi_C$ when $V \leq V_{fb}$, and $\Delta E_C = q\phi_C + q(V - V_{fb})$, when $V > V_{fb}$, A_C^* is Richardson's constant, and T_C is the absolute temperature of the cathode. The flat-band voltage V_{fb} is defined as

$$V_{fb} = \phi_C - \phi_A, \quad (13)$$

where ϕ_A is the work function of the anode material and

$$\phi_C = \frac{1}{q} (E_c - E_F + \chi_C) \quad (14)$$

is the work function and χ_C the electron affinity of the cathode material. The density of the anode current, which corresponds to electrons emitted from the anode, is given by

$$J_A = A_A^* T_A^2 \exp\left(-\frac{\Delta E_A}{k_B T_A}\right), \quad (15)$$

where $\Delta E_A = q\phi_A + q(V_{fb} - V)$ when $V \leq V_{fb}$, and $\Delta E_A = q\phi_A$, when $V > V_{fb}$, A_A^* is Richardson's constant of the anode, and T_A is the absolute temperature of the anode. We assume that all the electrons emitted from the cathode are collected by the anode and vice versa:

$$J = J_C - J_A. \quad (16)$$

The flat band voltage V_{fb} is an important parameter for the efficiency of the PETE device. At voltages V above V_{fb} the additional energy barrier $q(V - V_{fb})$ for the electrons emitting from the cathode appears (see Eq. (12)). This decreases J_C considerably. At voltages V below V_{fb} the electrons emitted from the anode are hindered by the energy barrier $q(V_{fb} - V)$ (see Eq. (15)). This allows J_A to be reduced by lowering V . In general, the highest output power will often be obtained near $V = V_{fb}$. However, when $T_C \gg T_A$, the high thermal energy of the cathode electrons allows the range $V > V_{fb}$ to be used as well.

Using $n_{eq} = N_c \exp[-(E_c - E_F)/(k_B T_C)]$ and Eqs. (7) and (12)–(16) the output electric current density can be written alternatively as

$$J = J_{\text{sun}} - J_{\text{dark}}, \quad (17)$$

where the photocurrent is given by

$$J_{\text{sun}} = \frac{q D_n}{L_n d} \Delta n_{\text{sun}}, \quad (18)$$

where

$$d = \begin{cases} \frac{q D_n N_c}{L_n A_C^* T_C^2} \exp\left(\frac{\chi_C}{k_B T_C}\right) + k & \text{for } V \leq V_{fb} \\ \frac{q D_n N_c}{L_n A_C^* T_C^2} \exp\left[\frac{\chi_C + q(V - V_{fb})}{k_B T_C}\right] + k & \text{for } V > V_{fb}. \end{cases} \quad (19)$$

The dark current is given by

$$J_{\text{dark}} = \frac{q D_n n_{eq}}{d L_n} \left\{ \frac{A_A^* T_A^2}{A_C^* T_C^2} \exp\left(\frac{q \Delta E_{\text{dark}}}{k_B T_C}\right) - 1 \right\} \quad (20)$$

where $\Delta E_{\text{dark}} = \phi_C + (V - \phi_C) T_C / T_A$ when $V \leq V_{fb}$, and $\Delta E_{\text{dark}} = V + \phi_A (1 - T_C / T_A)$, when $V > V_{fb}$. The dark current is the electric current that flows through the device when there is no illumination. Under illumination it usually decreases the total current, thus it should be eliminated. This can be done by choosing V optimally. However, if T_A is very low, the direction of J_{dark} can change, and the device harvests energy also from the thermal energy of cathode electrons similarly as a thermionic converter.

Eqs. (18) and (19) show that in order to maximize J_{sun} χ_C and k should be as small. On the contrary, then J_{dark} will also increase. J_{sun} can be increased and J_{dark} decreased by increasing T_C . J_{dark} can be reversed by having high ϕ_A and low ϕ_C (this will reduce V_{fb}). In addition, T_A and A_A^* should be small and T_C and A_C^* should be large.

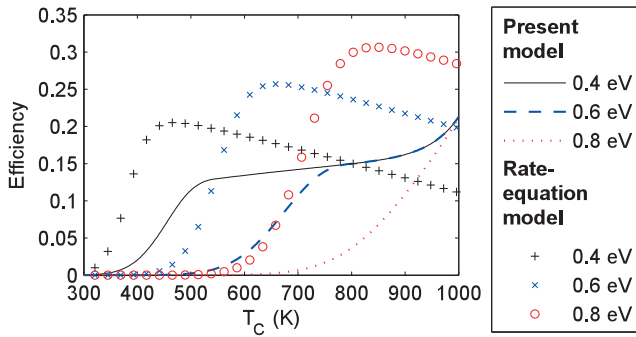


FIG. 3. Efficiencies of PETE devices with silicon cathodes with various electron affinities χ_C as functions of the cathode temperature T_C calculated using the numerical model with $N_A = 10^{18} \text{ cm}^{-3}$ and $W = 5 \mu\text{m}$ and without surface recombination at the concentration of 1000 suns. The results from the rate-equation model² were calculated with $E_g(T) = 1.12 \text{ eV}$.

III. RESULTS AND DISCUSSION

The semi-analytical model, Eqs. (8), (11), and (17)–(20), applies in the low injection condition ($\Delta n \ll p_{eq}$) with a P-type cathode material ($p_{eq} \gg n_{eq}$)⁵. The numerical calculations were performed using Eqs. (3)–(6) and (12)–(16). In both models V was optimized numerically for maximum output power. The AM1.5 direct+circumsolar spectrum applicable to solar concentrators was used in the calculations. We use $\langle 111 \rangle$ silicon as the cathode surface, for which³ $A_C^* = 264 \text{ A/cm}^2/\text{K}^2$. For the material parameters of the anode we use the same values as Schwede et al.², $\phi_A = 0.9 \text{ V}$ and $A_A^* = 120 \text{ A/cm}^2/\text{K}^2$. T_A was set at 573.15 K in order the heat engine potentially coupled to the anode to have a reasonably high efficiency^{10,11}. We also assume $R_{FS} = 0$ and $R_{BS} = 1$ for simplicity. The effect of R_{BS} , however, is not very large (see below), since it has an effect only on the absorption of low energy photons.

The efficiencies of PETE devices with various values of χ_C are plotted as functions of T_C in Fig. 3. They increase with increasing T_C and decreasing χ_C due to the increase of J_C . Using $R_{BS} = 0$ instead reduces the efficiency from 13.0 % to 11.7 % at 550 K in the case $\chi_C = 0.4$.

Fig. 3 shows also the efficiencies given by the simple rate-equation model², which assumes that all photons with energy greater than E_g are uniformly absorbed in the cathode. Only the uniform radiative recombination is taken into account with a general model based on the black-body radiation. At low T_C the rate-equation model suggests much higher efficiencies than the present more complete model. This is mostly due to the facts that all the possible photons are absorbed and the Auger recombination is not included in the rate-equation model.

The efficiency is a balance between many opposing effects, which depend on N_A and W : Increasing N_A increases V_{fb} which increases the efficiency. On the other hand, high N_A reduces the efficiency due to the Auger

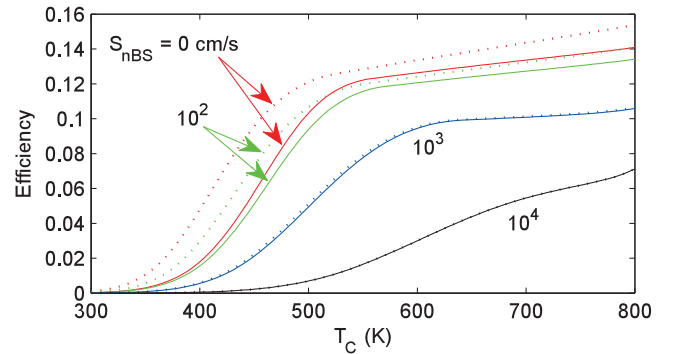


FIG. 4. Efficiency of a PETE device with a silicon cathode and various back-surface recombination velocities S_{nBS} as function of the cathode temperature T_C calculated using the numerical (solid lines) and semi-analytical (dotted lines) models with $S_{nFS} = 10^2 \text{ cm/s}$, $\chi_C = 0.4 \text{ eV}$, $N_A = 10^{18} \text{ cm}^{-3}$, and $W = 5 \mu\text{m}$ at the concentration of 1000 suns.

recombination which is proportional to N_A^2 . The effect of the bulk recombination can be reduced by decreasing W , but then some of the photons will not be absorbed. Although $5 \mu\text{m}$ is already small thickness for a silicon absorber, but, if W is increased to $50 \mu\text{m}$ while keeping N_A constant, the efficiency reduces from 13.0 % to 8.4 % at 550 K in the case $\chi_C = 0.4 \text{ eV}$. At high T_C the efficiency curves of the present model unite regardless of the differences in χ_C . The reason for this is that the total current does not depend on χ_C in this range: When $T_C \gg T_A$ the range $V > V_{fb}$ can be utilized and the output current density can be written using Eqs. (12)–(16) as $J = A_C^* T_C^2 \exp[(E_{F,n} - E_F - qV - q\phi_A)/(k_B T_C)] - A_A^* T_A^2 \exp(-q\phi_A/k_B T_A)$. The rate-equation model does not behave like this at high T_C , because Δn decreases much faster with increasing T_C than in the present model. This is caused mostly by the differences in the modeling of recombination and the narrowing of the band gap with increasing T_C which is taken into account only in the present model. The latter effect enhances both photogeneration and thermal generation of electrons, which causes the apparent efficiency increase at $T_C > 800 \text{ K}$.

The effect of S_{nBS} on the efficiency of the PETE device is shown in Fig. 4: Even a low value of S_{nBS} reduces the efficiency remarkably. Similar results were also obtained with various values of S_{nFS} . The efficiency is more sensitive to S_{nFS} than S_{nBS} because photogeneration is much stronger near the front surface than near the back surface. The semi-analytical model is in a very good agreement with the numerical model when the recombination velocities are $\geq 1000 \text{ cm/s}$ since the injection level is below 0.1 at $T_C > 550 \text{ K}$. In the low-injection conditions achieving surface recombination velocities less than 100 cm/s requires usually use of back surface field structures³. However, the surface recombination velocity decreases rapidly when the injection level is increased³ and values below 2 cm/s can easily be reached at injection level of unity (details depend on the properties of

the surface states)⁵. Therefore, the case of zero surface recombination can actually be realistic for a PETE device.

IV. CONCLUSIONS

In summary, we have built a theoretical model for PETE devices. Our model takes electron diffusion, inhomogeneous photogeneration, and bulk and surface recombination into account. In comparison to the rate equation model of Ref. 2 our model predicts different dependency of efficiency on such parameters as cathode electron affinity and temperature. In most cases our model also predicts lower efficiency. Especially, the surface recombination present on real surfaces can reduce the efficiency to extremely low values. However, the surface recombination might have only a very weak effect on the performance, since the PETE device works often in the high-injection conditions where the surface recombination can be rather small⁵. We finally point out that the realization of the PETE device requires choices of many parameter values and materials which should all be optimized. In addition, the heat balance between the PETE device and the heat engine coupled to the anode, which was not considered in this article, should be managed as well. Full optimization with heat balance modelling will be left for future studies.

ACKNOWLEDGMENTS

Fruitful discussions with J. Tervo, J. Ahopelto, K. Reck, O. Hansen, and P. Kuivalainen are gratefully acknowledged. This work has been financially supported by Nordic Energy Research (project HEISEC) and by the Academy of Finland (grant nr. 252598).

- ¹S. A. Kalogirou, *Solar Energy Engineering – Processes and Systems* (Elsevier, New York, USA, 2009).
- ²J. W. Schwede, I. Bargatin, D. C. Riley, B. E. Hardin, S. J. Rosenthal, Y. Sun, F. Schmitt, P. Pianetta, R. T. Howe, Z.-X. Shen, and N. A. Melosh, *Nature Materials* **9**, 762 (2010).
- ³S. M. Sze, *Physics of Semiconductor Devices*, 2nd ed. (Wiley-Interscience, New York, USA, 1981).
- ⁴P. P. Altermatt, *J. Comput. Electron.* **10**, 314 (2011).
- ⁵D. K. Schroder, *Semiconductor material and device characterization*, 3rd ed. (Wiley-Interscience, Hoboken, USA, 2006).
- ⁶P. P. Altermatt, J. Schmidt, G. Heiser, and A. G. Aberle, *J. Appl. Phys.* **82**, 4938 (1997).
- ⁷S. Reggiani, M. Valdinoci, L. Colalongo, M. Rudan, and G. Baccarani, *VLSI Design* **10**, 467 (2000).
- ⁸K. Rajkanan, R. Singh, and J. Shewchun, *Solid-State Electron.* **22**, 793 (1979).
- ⁹M. A. Green, *Solar Cells – Operating Principles, Technology and System Applications* (The University of South Wales, Kensington, NSW, Australia, 1982).
- ¹⁰W. R. Wagar, C. Zamfirescu, and I. Dincer, *Energy Conv. Management* **51**, 2501 (2010).
- ¹¹A. Kribus and G. Mittelman, *J. Solar Energy Eng.* **130**, 011001 (2008).
- ¹²T. Guo, *J. Appl. Phys.* **72**, 4384 (1992).